



12th International Conference on Vibration Problems, ICOVP 2015

On safety assessment and base isolation of heavy non-structural monolithic objects

Andrea Chiozzi^{a*}, Michele Simoni^a, Antonio Tralli^a

^aEngineering Department, University of Ferrara, Ferrara, ITALY

Abstract

Under seismic actions heavy non-structural objects, which are usually placed at the top of existing constructions, may constitute a danger to human lives and a considerable loss for world heritage. In this contribution, safety assessment of non-structural monolithic objects is discussed through the illustration of a case study, which concerns seismic protection of eleven ancient marble decorative pinnacles placed at the top of a three-arched masonry city gate in Ferrara (ITALY). A method for assessing the safety of the underlying masonry structure under the action of seismic excitations is outlined and the amplification of the ground motions due to the presence of such structure is evaluated.

© 2016 The Authors. Published by Elsevier Ltd. This is an open access article under the CC BY-NC-ND license (<http://creativecommons.org/licenses/by-nc-nd/4.0/>).

Peer-review under responsibility of the organizing committee of ICOVP 2015

Keywords: Seismic Isolation, Masonry, Monolithic Objects, Non-structural Elements.

1. Introduction

Many research efforts have been devoted, in the past, to devise effective seismic protection systems for heavy artwork, sculptures, pinnacles, merlons (see e.g. Fig. 1b), which do not have a structural function but belong to world heritage and, in many cases, have an inestimable value; for an introduction to this subject the reader is addressed to [1], [2]. The aim of the present contribution is to examine more in-depth some aspects related to the case study of the seismic protection through base isolation of eleven ancient marble pinnacles placed at the top of the three-arched masonry city gate in Ferrara, Italy, portrayed in Fig. 1a. The three-arched masonry city gate was built in Ferrara Italy

* Corresponding author. Tel.: +39-3474027959;

E-mail address: andrea.chiozzi@unife.it

between 1703 and 1704 a.C (Fig. 1a). The marble pinnacles placed at the top of the gate have mainly a decorative purpose and their slenderness, coupled with their considerable mass, makes them highly vulnerable to seismic actions so that they cannot be considered safe. This case study has been recently described and analyzed by the authors in [3, 4], where a specific base isolation system based on the use of multiple double concave curved surface steel sliders has been devised; nevertheless, in order to assess the effectiveness of the isolation system in preventing rocking and overturning of the pinnacles, an accurate evaluation of the dynamical response of the underlying masonry construction can be helpful.



Fig 1. (a) Three-arched masonry city gate, Corso Giovecca, Ferrara, Italy; (b) Masonry merlons belonging to the Castle of San Felice sul Panaro, Italy, (orthophoto).

For this reason and differently from the previous works, the present paper is mainly focused on the investigation of the dynamical behavior of the three-arched masonry construction and of the amplification of the ground motions due to its presence. The definition of suitable incremental constitutive relationships that correctly accounts for all the dissipation mechanisms of masonry is a completely open research subject. Recently, simplified and/or heuristic approaches such as macroelement models [5], rigid body and spring models [6] combined finite and discrete elements [7] have been successfully used for seismic analyses of unreinforced masonry structures. For the problem at hand, it can be shown that overturning of the pinnacles occurs when the masonry structure, though undergoing damage, is still very far from collapse [3]. Thus, a time-history analysis of the structure is carried out assuming an elastic behavior of masonry, in which damping coefficients have been suitably defined. The paper is organized as follows. In Section 2 the underlying three-arched masonry city gate structure is characterized, performing a natural frequency analysis and pushover analyses. In particular modal pushover analysis (MPA) [8, 9] have been employed. In Section 3, the evaluation of the amplification effect of the underlying masonry structure has been discussed.

2. Characterization of the three-arched masonry structure

2.1. In-plane push-over analysis

Employing the finite-element analysis code DIANA [10], in-plane capacity curve for the masonry structure has been determined through a non-linear incremental finite element analysis, using a force distribution proportional to the principal in-plane vibration mode, which has been obtained through a natural frequency analysis. The finite element model used for the analysis is shown in Fig. 2a, along with the main four modal shapes. A total strain elastic-plastic damaging constitutive law is assigned. The obtained in-plane capacity curve (shown in Fig. 3a) relates the total shear force Fb applied at the base of the structure with the in-plane displacements d_c of a control point which has been chosen as the medial point placed on one of the short sides of the construction, at a height of 3.00 m.

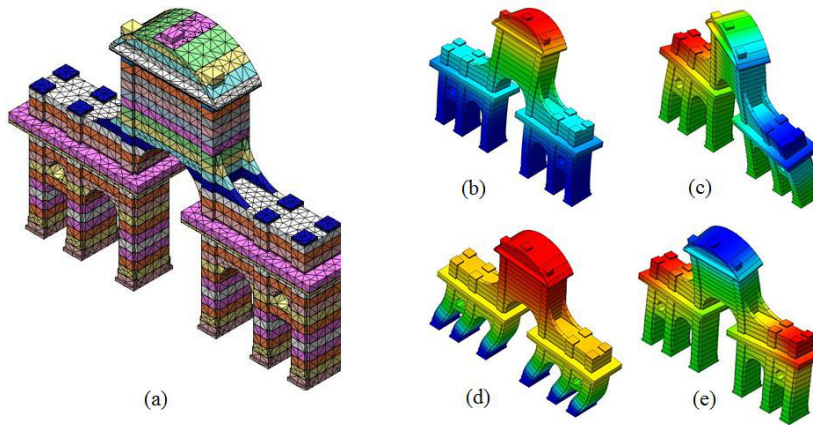


Fig 2. (a) Finite element model of the three-arched masonry city gate for natural frequency analysis; the first four vibration modes: (b) translational mode in the out-of-plane direction, (c) torsional mode, (d) translational mode in the in-plane direction, (e) partial translational model in the out-of-plane direction.

Then, in-plane pushover analysis have been conducted. According to [11] an equivalent single d.o.f. structural system is determined starting from the original multi-d.o.f. capacity curve. The capacity curve of the equivalent system is then approximated by a bilinear capacity curve with an elastic-plastic like behavior (Fig. 3b). The equivalent single d.o.f. System is characterized by an initial stiffness k^* and a yield force F_y^* . The elastic period of the bilinear system is given by:

$$T^* = 2\pi \sqrt{\frac{m^*}{k^*}} \tag{1}$$

where $m^* = \Phi^T \mathbf{M} \Phi$, in which \mathbf{M} is the mass matrix of the real system, Φ is the vector corresponding to the principal mode of the real system normalized by posing $d_c = 1$ and τ is the vector representing the considered seismic direction. In case $T^* \geq T_c$, the demand in terms of displacements for the inelastic system is assumed equal to that of an elastic system with the same period:

$$d_{\max}^* = d_{e,\max}^* = S_{De}(T^*) \cdot \tag{2}$$

In case $T^* < T_c$ the demand in terms of displacements for the inelastic system is greater than that of an elastic system with the same period and is given by the following expression:

$$d_{\max}^* = \frac{d_{e,\max}^*}{q^*} \left[1 + (q^* - 1) \frac{T_c}{T^*} \right] \tag{3}$$

where $q^* = S_e(T^*)m^* / F_y^*$ is the ratio between the elastic response force and the yield force for the equivalent system. Pushover analysis is satisfied if displacement demand d_{\max}^* is less than displacement capacity d_u^* of the equivalent single d.o.f. system. The procedure described above can be translated graphically by comparing the bilinear capacity curve of the single d.o.f. equivalent system (whose ordinates must be divided by m^*) with the elastic response spectrum in terms of spectral acceleration and displacement (ADRS) which is given by [11] depending on the location and soil category. In this case it is easily seen that $T^* < T_c$. Therefore, the intersection point provides the value for displacement demand.

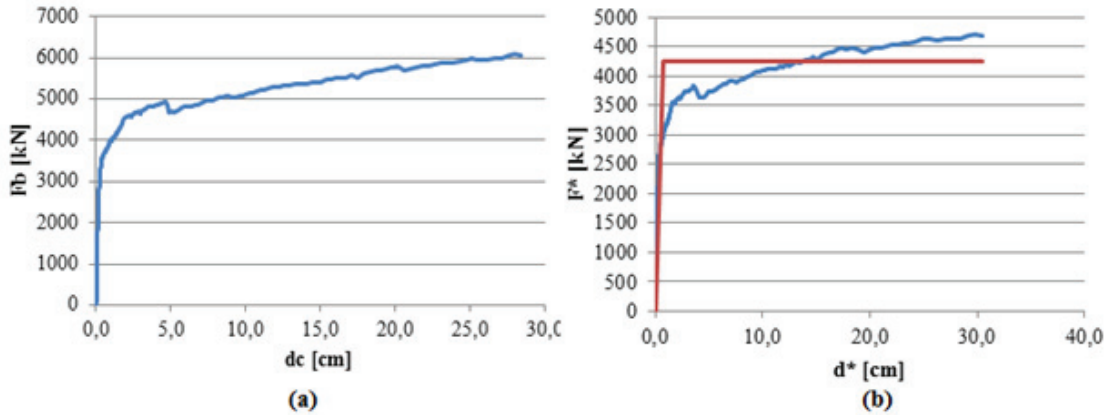


Fig. 3. (a) Capacity curve of the original masonry structure the in-plane direction (b) Capacity curve of the equivalent single d.o.f. system and its bilinear approximation.

As shown in Fig. 4(a) the structure remains in its elastic range for the design seismic action and d_{max}^* is equal to 0.6cm, which is widely less than displacement capacity. Correspondent crack-pattern is reported in Fig. 4b.

2.2. Out-of-plane modal pushover analysis

According to [12], since participating mass for the principal out-of-plane mode is less than 60%, non-linear static analysis is not allowed and in the following the recently proposed Modal Pushover Analysis (MPA) [8], which takes into account several vibration modes in the out-of-plane direction, has been applied. MPA is based on the superposition of uncoupled and suitably chosen modal responses. In the present case study, two out-of-plane eigenvectors have been chosen: the first and the fourth mode so that total out-of-plane participating mass is equal to 80.98 %. At first, standard pushover analysis have been separately performed for each of the selected vibration modes, obtaining for each mode the displacement demand d_{max}^* for the equivalent single d.o.f. oscillator. Then, the maximum displacement demand for the control point d_c in the real multi-d.o.f. system can be computed through the following relation:

$$d_{max} = \Gamma \cdot d_{max}^* \tag{4}$$

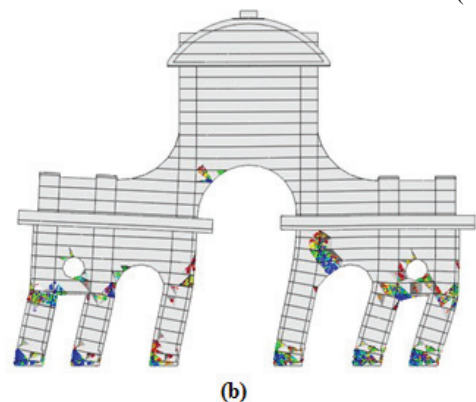
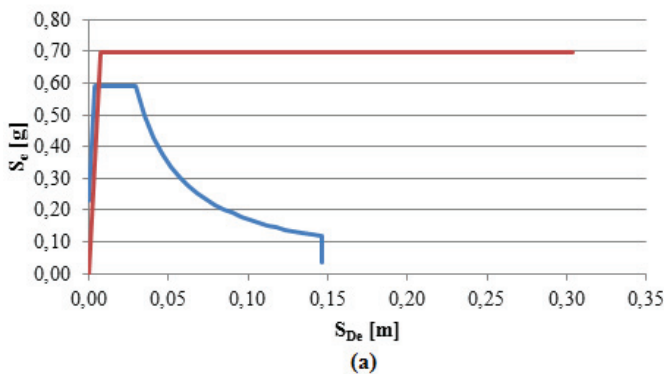


Fig 4. (a) Graphical determination of the displacement demand by comparing the bilinear capacity curve of the single d.o.f. equivalent system (red line) with the elastic response spectrum in terms of spectral acceleration and displacements (blue line). (b) Crack-pattern obtained with an in-plane incremental non-linear analysis with DIANA for a displacement level equal to the displacement demand.

where r is the modal participation factor and the results will be finally combined according to MPA procedure.

A first standard pushover analysis has been conducted starting from an inertial force distribution proportional to the shape of the first vibration mode. A force-displacement capacity curve for the masonry structure has been computed. The top of the construction has been chosen as control point. From this curve, the capacity curve of a single d.o.f. system equivalent to the original multi-d.o.f. system has been determined and a bilinear approximation has been defined (Fig. 5a). From Fig. 5b, which compares the single d.o.f. bilinear capacity curve with the elastic response spectrum, it is possible to infer that the structure goes beyond its elastic range and that $T^* > T_C$. Correspondent crack-pattern is reported in Fig. 5c. The ductility factor q^* is equal to 2.1 whereas the displacement demand for the single d.o.f. system d_{max}^* is equal to 3.3 cm. Using Eq. 1.4, it is possible to obtain the displacement demand for the control point in the original structure d_{max} , equal to 6.16 cm. Analogously, a further standard pushover analysis has been conducted starting from an inertial force distribution proportional to the shape of the fourth vibration mode.

Again, the top of the construction has been chosen as control point. From this curve, the capacity curve of a single d.o.f. system equivalent to the original multi-d.o.f. system has been determined and a bilinear approximation has been defined (Fig. 6a). From Fig. 6b, it is possible to infer that the structure remains within its elastic range and that $T^* < T_C$. Therefore, the ductility factor q^* is equal to 1 whereas the displacement demand for the single d.o.f. system d_{max}^* is equal to 0.6 cm. Finally, using Eq. 1.4, it is possible to obtain the displacement demand for the control point in the original structure d_{max} , which results equal to 0.6 cm. Correspondent crack-pattern is reported in Fig. 6c. MPA requires that results obtained from separate pushover analysis for each selected eigenvector be combined using SRSS:

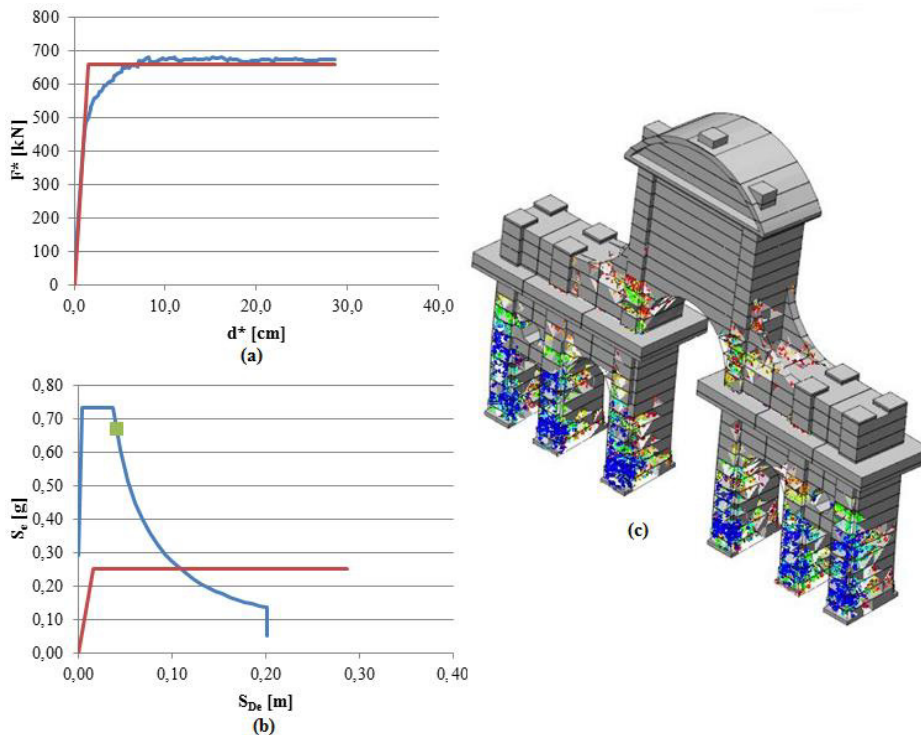


Fig. 5. (a) Capacity curve of the equivalent single d.o.f. system and its bilinear approximation for a force distribution proportional to the first mode. (b) Graphical determination of the displacement demand by comparing the bilinear capacity curve of the single d.o.f. equivalent system (red line) with the elastic response spectrum in terms of spectral acceleration and displacements (blue line). (c) Crack-pattern obtained with a incremental non-linear analysis with DIANA for a displacement level equal to the displacement demand.

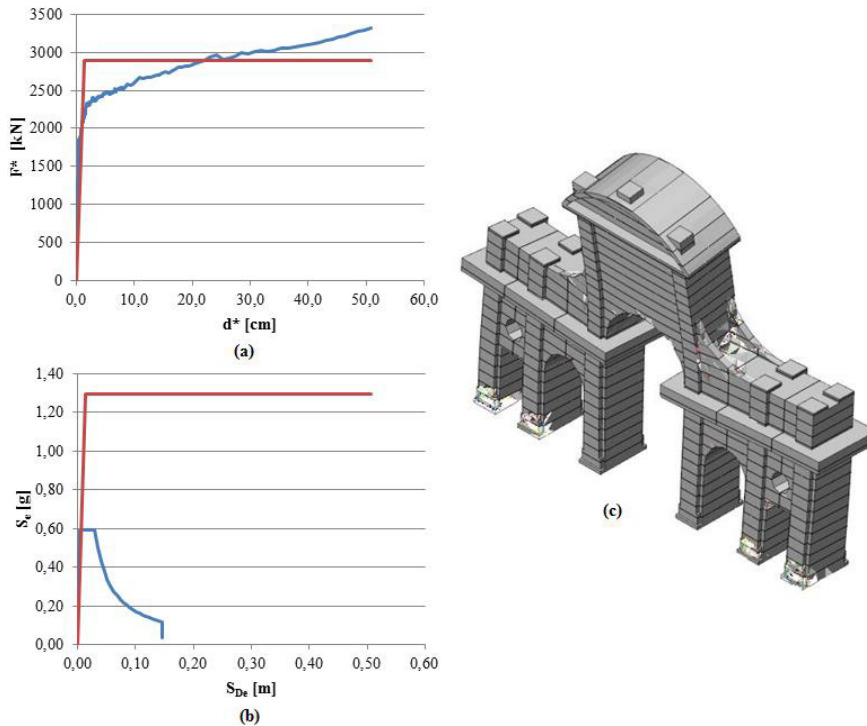


Fig. 6. (a) Capacity curve of the equivalent single d.o.f. system and its bilinear approximation for a force distribution proportional to the fourth mode. (b) Graphical determination of the displacement demand by comparing the bilinear capacity curve of the single d.o.f. equivalent system (red line) with the elastic response spectrum in terms of spectral acceleration and displacements (blue line). (c) Crack-pattern obtained with an incremental non-linear analysis with DIANA for a displacement level equal to the displacement demand.

$$d_0 = \left(\sum_{i=1}^N d_{i0}^2 \right)^{1/2} \tag{5}$$

where d_{i0} is the displacement profile vector for the i -th vibration mode and N is the number of vibration modes considered. Three different displacement profiles have been considered, respectively defined along external columns (P1), intermediate columns (P2) and internal columns (P3) of the three-arched masonry structure. For each vibration mode, displacement profiles have been obtained from pushover analyses, which give the maximum displacement the control point undergoes under the action of the prescribed seismic action. Finally, it is possible to compute the combined value of the ductility factor q as a weighted average of the ductility factors of the two considered modes, the weights being the activated mass by each mode:

$$q = \frac{q_1^* m_1^* + q_4^* m_4^*}{m_1^* + m_4^*} . \tag{6}$$

Ductility factor q turns out equal to 1.59, suggesting a substantially elastic behavior.

3. Numerical evaluation of the amplification effect

In order to evaluate the dynamic response of the isolated pinnacles at the top of the masonry construction through non-linear time-history analyses, the amplification effect of the ground motions due to the underlying structure has to be quantified.

3.1. Definition of spectrum compatible ground motions

As required by [12], ground motions compatible with earthquake design spectra must be selected in order to use time-history dynamic analyses to assess the structural safety of the system. To this aim, a set of seven different ground accelerograms compatible with the earthquake design spectrum of the site, defined in [12], has been generated starting from seven natural accelerograms. Initially chosen accelerograms are scaled, so that the average of the spectral ordinates obtained for each scaled accelerogram must not differ from the elastic design earthquake spectrum of more than 10%, in a range of periods which has to be chosen as the largest between $0,15 \text{ s} - 2 \text{ s}$ and $0,15 \text{ s} - 2T_1 \text{ s}$, where T_1 is the fundamental period of the structure.

3.2. Evaluation of the amplification effect

For each spectrum compatible ground accelerogram, applied at the base of the structure as a forcing action, two different time-history dynamic analyses of the three-arched masonry city gate have been carried out, one with the ground accelerations applied in the in-plane direction and one with the ground accelerations applied in the out-of-plane direction. Therefore, fourteen analyses have been conducted.

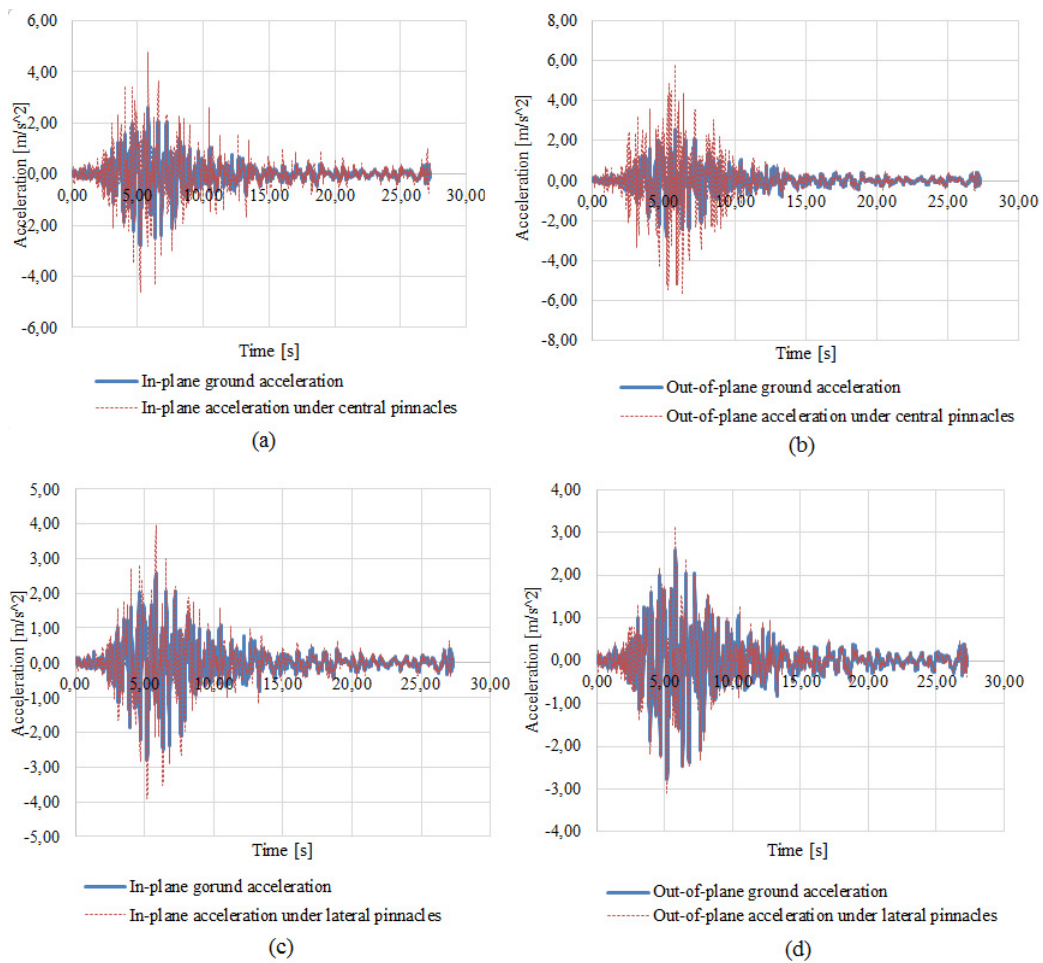


Fig. 7 Amplification of the base seismic action 378ya due to the masonry structure on central pinnacles in the in-plane (a) and out-of-plane (b) directions and on lateral pinnacles in the in-plane (c) and out-of-plane (d) directions.

By observing that the three arched structure will behave nearly elastically, masonry has been modeled as a linear visco-elastic material with a Raleigh damping model. This means that the global damping matrix is assumed as a linear combination of the global stiffness and mass matrices through constants of proportionality which depend on the frequencies ω_1 and ω_2 of the two principal modes. A number of technical papers deal with the determination of the corresponding damping coefficients ξ_1 and ξ_2 . An experimental determination is described in [14] whereas in [15] the values of 0.05 and 0.10 respectively for ξ_1 and ξ_2 are suggested for masonry structures. An alternative way has been presented in [16] in which damping coefficients are determined following an iterative numerical procedure. More precisely, the equivalent viscous damping coefficient is assumed varying with the maximum displacement level reached by the structure during earthquake solicitation. Thus, a relation between the equivalent viscous damping coefficient and the maximum displacement that the structure can reach under seismic actions is determined starting from the capacity curves of the masonry structure and the definition of a hysteretic force-displacement law for the equivalent single d.o.f. system, which allows to evaluate the response under cyclic loading. A series of time-history dynamic analyses on the single d.o.f. equivalent system allows to determine a set of values for ξ_1 and ξ_2 in the ranges 0.02-0.07 and 0.8-1.2 respectively, that are in agreement with the ones suggested in [15], which have been therefore assumed. Once defined the damping parameters, the response of the structure in terms of acceleration at the base of both lateral and central pinnacles have been determined. This response represents the design seismic accelerogram to be applied at base of the isolated pinnacles in order to assess the effectiveness of the isolation system. Fig.7(a)-(b) depicts a comparison between the accelerogram 378ya applied at the ground level in the two main directions and the corresponding accelerogram computed at the level of central pinnacles. Fig.7(c)-(d) depicts a comparison between the accelerogram 378ya applied at the ground level in the two main directions and the corresponding accelerogram computed at the level of lateral pinnacles.

Acknowledgements

The authors gratefully acknowledge the financial contribution of Fondazione Fornasini.

References

1. McGavin, G.L.: Earthquake protection of essential building equipment. John Wiley and Sons (1981).
2. Agbabian, M.S., Masri, S.F., Nigbor, R.L., Ginell, W.S.: Seismic damage mitigation concepts for art objects in museums. In: Proceedings of 9th world conference on earthquake engineering, Tokyo-Kyoto, Japan (1988).
3. Chiozzi, A., Simoni, M., Tralli, A.: Safety assessment and base isolation of heavy non-structural monolithic objects at the top of a masonry monumental construction. *Materials and Structures*, (2015). DOI 10.1617/s11527-015-0637-z.
4. Chiozzi, A., Simoni, M., Tralli, A.: Seismic protection of heavy non-structural monolithic objects at the top of a historical masonry construction through base isolation. In: Proceedings of 5th ECCOMAS Thematic Conference on Computational Methods in Structural Dynamics and Earthquake Engineering, Crete Island, Greece (2015).
5. Penna, A., Lagomarsino, S., Galasco, A.: A nonlinear macro-element model for the seismic analysis of masonry buildings. *Earthquake engineering & Structural Dynamics*, 43, 159-179 (2014).
6. Casolo, S., Peña, F.: Rigid element model for in-plane dynamics of masonry walls considering hysteretic behavior and damage. *Earthquake Engineering and Structural Dynamics*, 36, 1029-48 (2007).
7. Nolic, Z., Smoljanovic, H., Zivaljic, N.: Seismic analysis of dry stone masonry structures based on combined finite-discrete element method. In: Proceedings of the 9th International Conference on Structural Dynamics, Porto, Portugal (2014).
8. Chopra, A.K., Goel, R.L.: A modal pushover analysis procedure for estimating seismic demands for buildings. *Earthquake Engineering and Structural Dynamics*, 31, 561-582 (2002).
9. Reyes, J.C., Chopra, A.K.: Three-dimensional modal pushover analysis of buildings subjected to two components of ground motion, including its evaluation for tall buildings. *Earthquake Engineering and Structural Dynamics*, 40, 1475-1494 (2011).
10. TNO-DIANA: DIANA, Finite Element Analysis. www.tnodiana.com (2015).
11. Repubblica Italiana: Circolare sulle "Nuove Norme Tecniche per le Costruzioni" di cui al DM 14/01/2008. S.O. n. 27, G.U. n. 47 (2009).
12. Repubblica Italiana: Norme Tecniche per le Costruzioni. S.O. n. 30 G.U. n. 29 (2008).
13. Gentile, C., Saisi, S.: Ambient vibration testing of historic masonry towers for structural identification and damage assessment. *Construction and Building Materials*, 21, 1311-1321 (2007).
14. Peña, F., Lourenço, P.B., Mendes, N., Oliveira, D.: Numerical models for the seismic assessment of an old masonry tower. *Engineering Structures*, 32, 1466-1478, (2010).
15. Nicolini, L.: Equivalent viscous damping and inelastic displacement for strengthened and reinforced masonry walls. Ph. D. Thesis, University of Trento (2012).